nzsee
NEW ZEALAND SOCIETY FOR EARTHQUAKE ENGINEERING

Multistage Friction Connections

J.C. Chanchí Golondrino, H.A. Coral Potosí
Universidad Nacional de Colombia, Departamento de Ingeniería Civil, Manizales – Caldas, Colombia.

G.A. MacRae
University of Canterbury, Civil and Natural Resources Engineering Department, Christchurch, New Zealand

ABSTRACT

Multistage friction connections (MFCs) are bolted connections for dissipating seismic energy while reducing peak displacements and encouraging recentring. MFCs comprise two symmetric friction connections co-linearly assembled. Each friction connection dissipates energy by sliding a slotted plate on high hardness shims placed either side of the slotted plate. One of these friction connections is assembled with fewer bolts than the other; thus, the MFCs ends are termed the weak and strong ends. MFCs have been recently proposed. However, to date, no experimental validation is available. This paper describes the assembly, sliding mechanism, and applications of MFCs in steel frames. Monotonic testing was undertaken on 3 MFCs assembled with tempered steel shims (hardness = 500BH), A36 steel slotted plates (F_y = 250MPa, F_u = 325MPa), and A325 bolts (F_y = 635MPa, F_u = 835MPa). Results show the MFCs force-displacement curve has two force steps representing the sliding of the slotted plate at the weak and strong ends. The ratio between these two forces, is the ratio between the number of bolts at the MFCs ends. The initial stiffness is steep and corresponds to the MFC axial stiffness without sliding. The second stiffness is less than the initial due to the combined action of the initial stiffness, and the bolt bending stiffness at the MFC weak end and resulting from bearing between the bolt and the slotted plate. These experimental results were used for proposing a simple model for the MFCs monotonic force-displacement curve.

KEY WORDS: Seismic Dissipation, Friction, Bolted Connection, Multistage Friction Connections

1 INTRODUCTION

Symmetric Friction Connections (SFCs) are bolted connections used to dissipate seismic energy (Grigorian and Popov 1994). SFCs can be assembled with a central slotted plate and two fixed plates, each fixed plate at one side of the slotted plate. To ensure stable hysteretic behaviour, high hardness shims are inserted between the slotted plate and the fixed plate (Chanchí et al. 2020). Testing of SFCs subassemblies, braces with SFC, and braced frames equipped with SFCs within the braces have demonstrated the hysteresis loop for SFCs and its application is almost rectangular (Grigorian and Popov 1994, Tremblay 1993, Fitzgerald 1989, Xie et al. 2018). As a result of this rectangular hysteresis loop, SFCs cannot provide dynamic self-centring (MacRae 1994), thus significant residual displacements may occur, which in combination with P – Δ effects may lead to the collapse of the structure. (MacRae 2021). To reduce this SFC undesirable behaviour, the idea of coupling in series two SFCs with different strength aiming to pinch the hysteresis loop has been recently

proposed and termed Multistage Friction Connections (MFCs) (MacRae 2021). However, to date, there is no experimental validation of MFCs. This paper describes results from experimental testing of MFCs and proposes a simple model for predicting the monotonic tensile force – displacement relationship for MFCs.

2 MATERIALS AND METHODS

2.1 MFCs Concept and applications

Multistage Friction Connections (MFCs) are bolted connections comprising two symmetric friction connections co-linearly assembled. Each symmetric friction connection is assembled with a slotted plate with high harness shims placed at both sides of the slotted plate. The slotted plates and the shims are sandwiched by two fixed plates, and clamped by high strength bolts, as shown in Figure 1a.

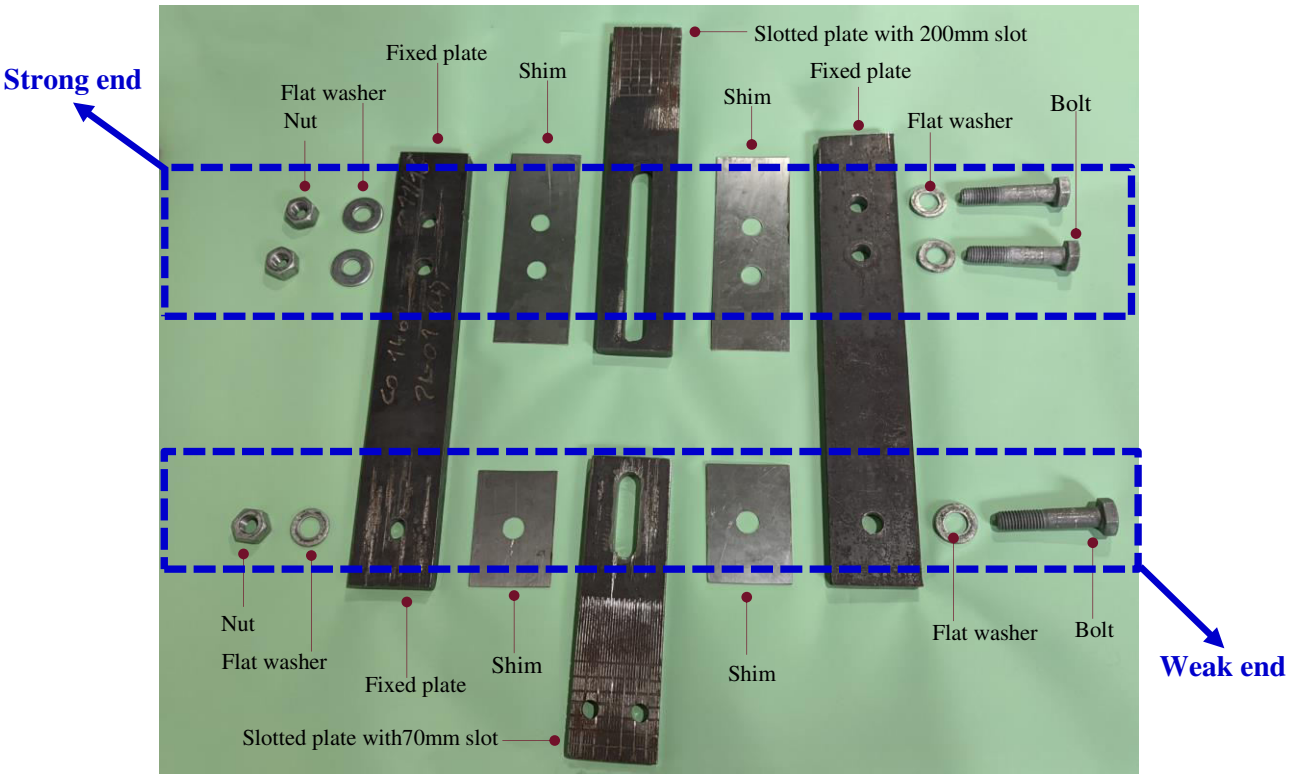

a. MFC components

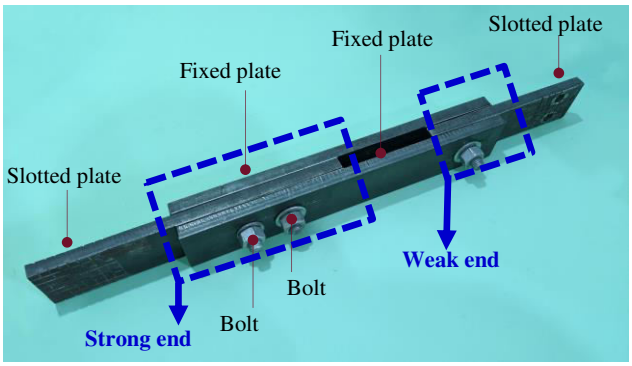

b. MFC assembly lateral view

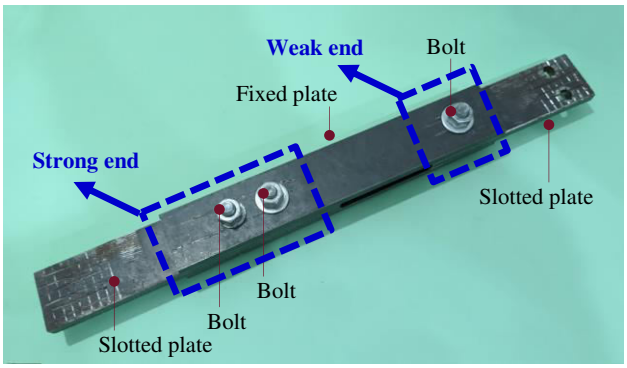

c. MFC assembly plan view

Figure 1: MFCs components and assembly

One of these friction connections is assembled with fewer bolts than the other; thus, the MFCs ends are termed the weak and strong ends, as shown in Figures 1b – c. In MFCs energy is dissipated as the slotted

plate at the weak end slides before the slotted plate at the strong end. MFCs are desirable because they can reduce peak displacements and encourage recentring, since the hysteresis loop shape can be pinched due to the in-series response of the two symmetric friction connection comprising the MFC.

MFCs can be used as seismic dissipaters for moment resisting frames or for braced frames. In moment resisting frames, MFCs can be installed at beam to column joints by welding a slotted plate on the column to assemble the MFC weak end, and by slotting the bottom flange of the beam to assemble the strong end, as shown in Figure 2a. In this application, the MFC dissipates seismic energy as the beam to column joint rotates producing sliding on the slotted plates. MFCs can be installed within braces by slotting the brace body and the gusset plate to assemble the weak and the strong end, respectively, as shown in Figure 2b. In this application**,** the MFC dissipates seismic energy as the brace elongates.

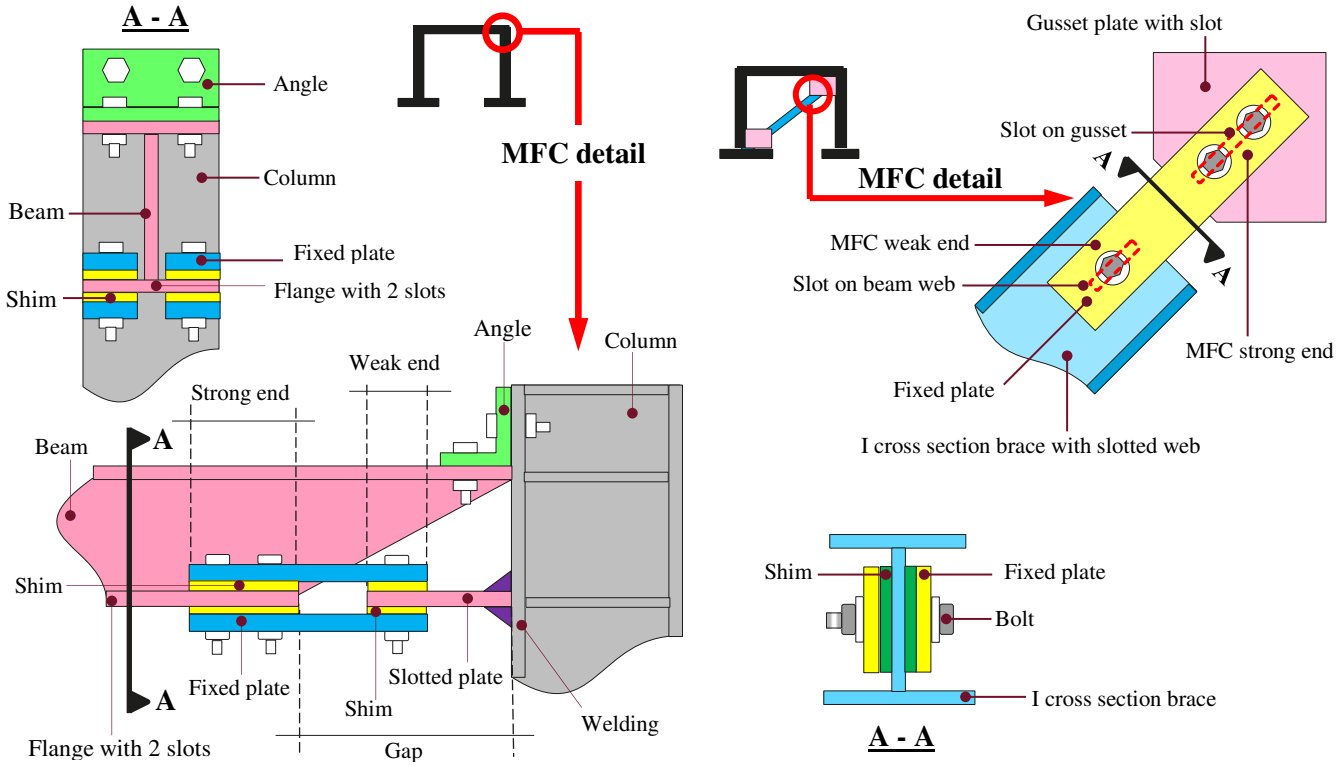

a. MFCs applications in beam-column joints *b. MFCs applications in braced frames*

Figure 2: MFCs applications in steel frames

2.2 MFCs Materials and Assembling Method

MFCs were assembled with A36 steel (F_y = 250MPa, F_u = 325MPa), A325 bolts (F_y = 635MPa, F_u = 835MPa), and tempered steel (hardness = 500BH). The fixed and slotted plates (i.e., with slots of 70mm and 200mm) were made of A36 steel with 16mm thickness, shims were of tempered steel with 2mm thickness, and bolts were of 16mm diameter and 63.5mm long. Bolts were assembled with two flat washers 3mm thick, one washer placed under the bolt head and the other washer under the nut. The two flat washers, the two fixed plates, the two shims, and the slotted plate comprising either the weak or the strong end had a bolt grip length of 58mm. Bolts were tensioned to the proof load, F_{proof}, of 85kN using the nut rotation method (Research Council on Structural Connections 2000). Since the ratio of the bolt length to the bolt diameter was less than 4, a nut rotation of 120º from the snug tight condition was used.

2.3 MFCs Monotonic Tensile Testing

MFCs were monotonically tested in tension in a universal MTS machine, and with the vertical setup shown in Figure 3a. The MFCs ends were grooved with a grid pattern of 1mm depth and by a length of 70mm, as shown in Figure 3b. This grooved grid pattern was provided to avoid any slip at the MFCs ends within the universal machine jaws. Three symmetric MFCs were tested, each MFC tested once, and with a velocity of 1mm/s and with a maximum displacement of 70mm.The maximum displacement of 70mm corresponded to 50% of the slot at the weak end (i.e., 35mm/70mm) since the bolts start moving from the centre of the slot and move to the end of the slot, plus 18% of the slot at the strong end (i.e., 35mm/200mm), thus, bearing of the bolt on the slotted plate only occurs at the weak end.

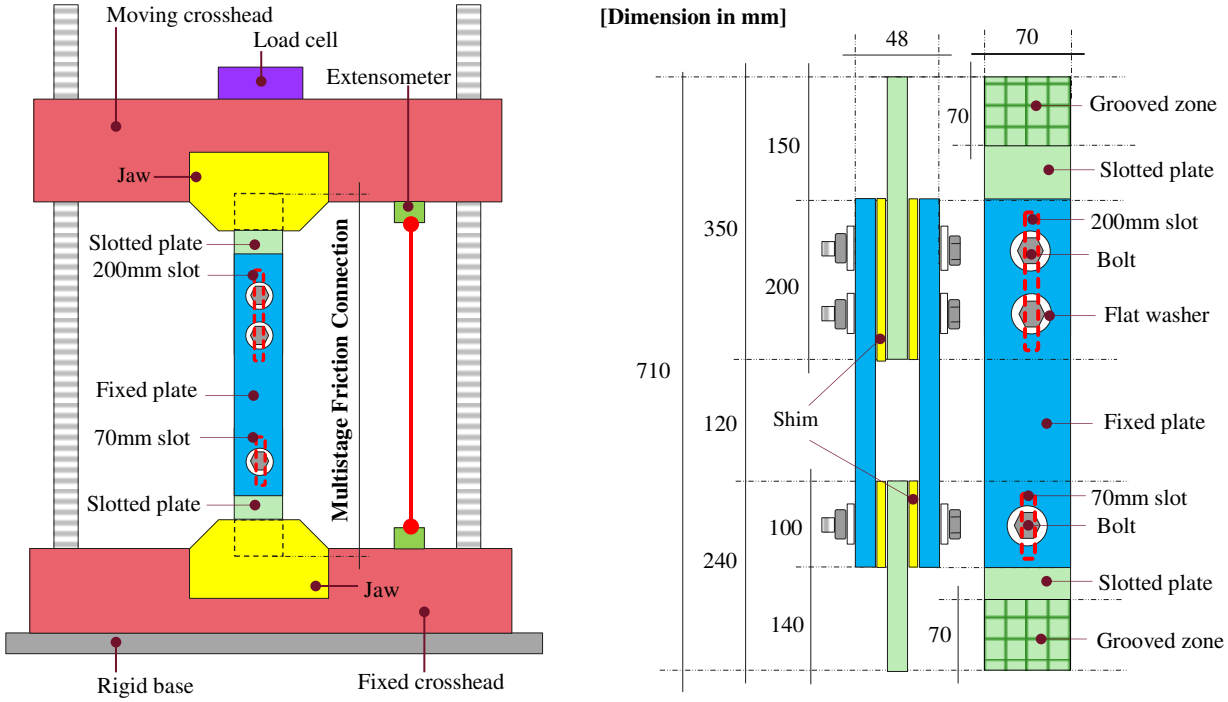

a. MFCs monotonic tensile testing setup *b. MFCs frontal and lateral view dimensions*

Figure 3: MFCs testing setup and MFCs frontal view

2.4 Angle of Friction and Material Friction Coefficient

The angle of friction θ is defined as the angle that activates the sliding of a body lying on an inclined plane (Popov 2017). The friction coefficient between two materials under gravity loads is termed here the material friction coefficient, μ, and it can be expressed in terms of θ (Popov 2017):

$$\boldsymbol{\mu = tan\theta} \tag{1}$$

Where, θ is the angle of friction in degrees. Figures 4a - b show a device to measure the angle of friction (Chanchí Golondrino, Moreno Castañeda, Restrepo Botero 2022). The device to measure the angle of friction comprises a platform that can be inclined by rotating a threaded rod, as shown in Figure 4c. The platform is equipped with a 3mm recessed hole, where a "sliding plate" plate of 70mm width, 100mm length and 5mm thickness, can be inserted. This plate becomes the sliding surface where friction occurs with the coupons. The coupons are 20mm wide, 30mm long, and 1.5mm thick. The sliding plate and the coupon correspond to the materials between which θ and μ can be obtained. θ can be obtained by rotating the threaded rod in the device until the sliding of the coupon is activated, and μ can be obtained through

Equation 1. In the test, the surfaces of the sliding plate and the coupon were cleaned with thin layer of acetone and a clean rag.

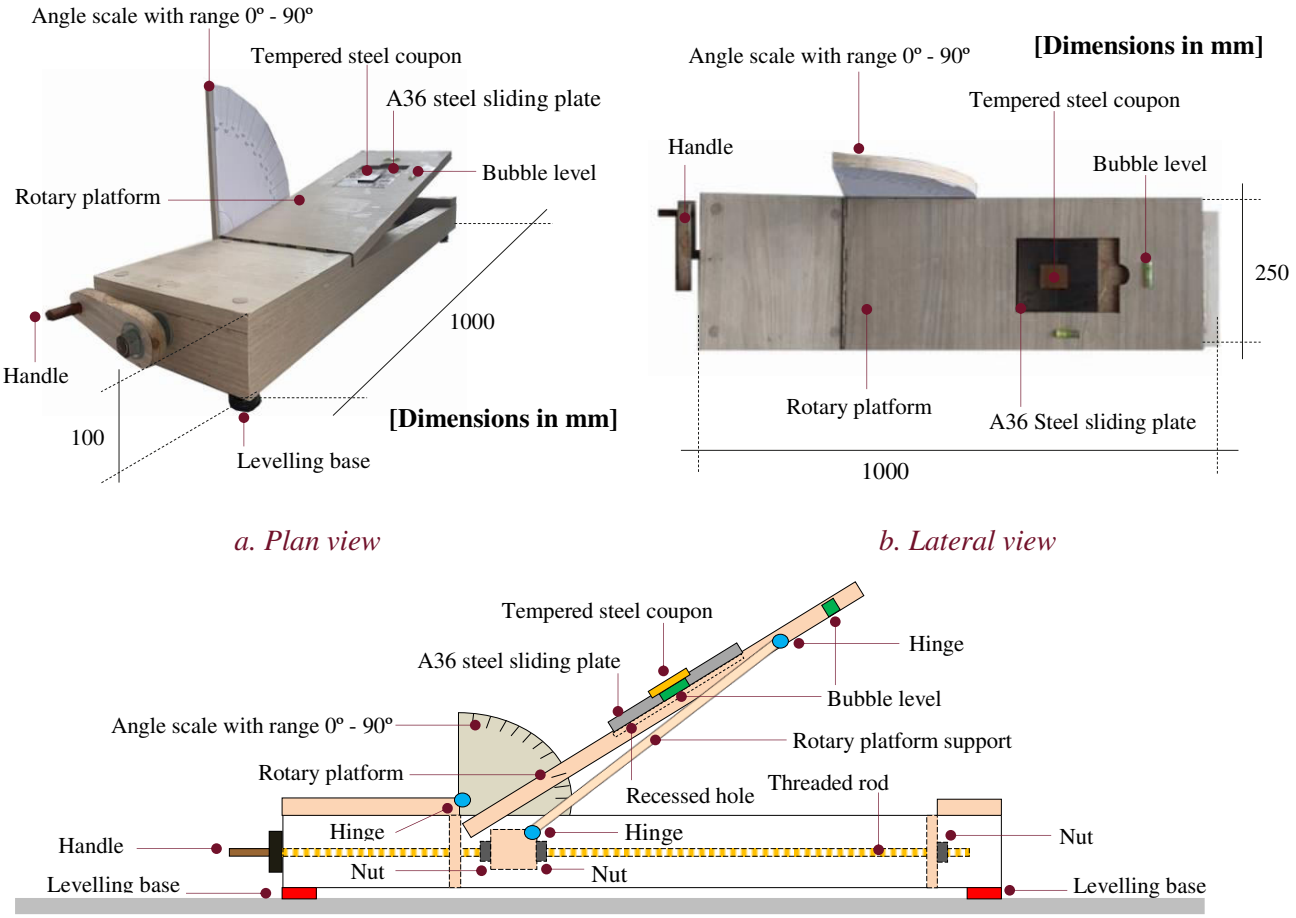

a. Plan view *b. Lateral view*

c. Lateral view idealization

Figure 4: Device to measure the angle of friction (Chanchí Golondrino, Moreno Castañeda, Restrepo Botero 2022)

2.5 Plate Axial Stiffness

The stiffness of a plate under a tensile axial load, k_a, is expressed:

$$k_a = \frac{AE}{L} \tag{2}$$

Where, for the plate, A is the cross-section area, E is the elastic modulus, and L is the length. In Equation 2, the bolt holes and/or slotted holes in the plate are ignored.

2.6 Bolt Bending Stiffness

In MFCs, after the sliding of the slotted plate at the weak end, the edge of the slotted hole reaches the bolt shank, thus bearing of the slotted plate on the bolt shank, and bolt bending occur, as shown in Figures 5a - b. The bolt in bending can be idealized as a beam under a joint load at the mid-span, and with a pinned support at the bolt head – fixed plate interface, and at the nut – fixed plate interface, as shown in Figure 5b. The bending stiffness of the bolt at the weak, k_b, can be expressed:

$$k_b = \frac{48E_bI_b}{g^3} \quad (3)$$

Where, for the bolt, E_b is the elastic modulus, I_b is the inertia, and g is the grip length outside of flat washers.

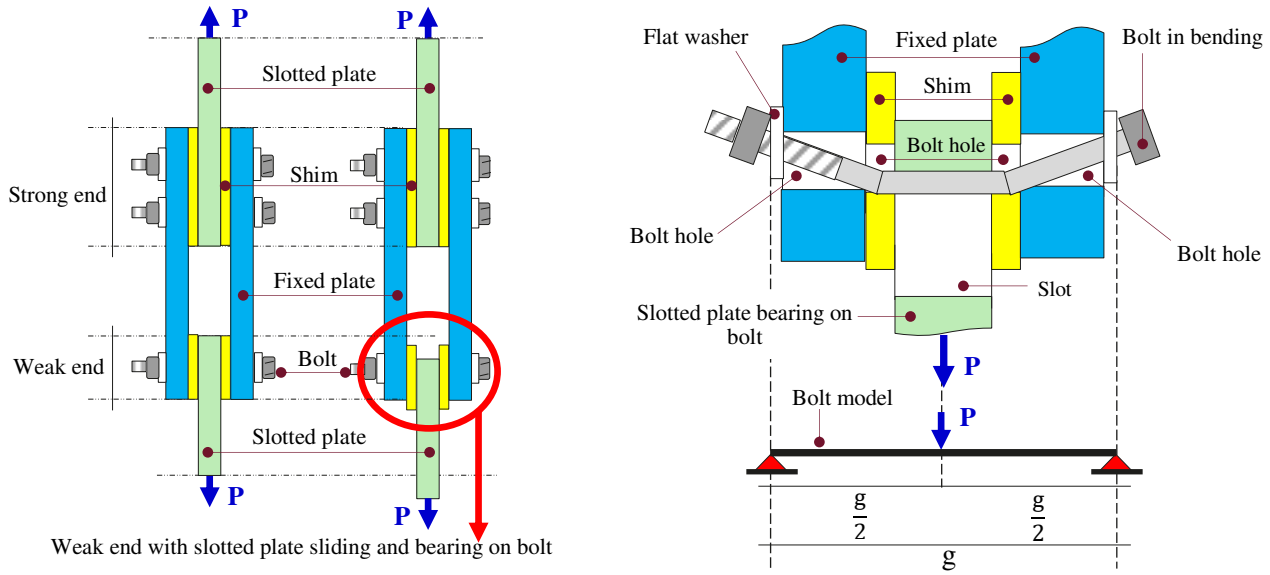

a. Sliding of the slotted plate at the MFC weak end *b. MFC weak end internal view*

Figure 5: Bolt in bending at the MFC weak end

3 RESULTS AND ANALYSIS

3.1 Monotonic Tensile Force – Displacement Curve

Figure 6 show the monotonic tensile force – displacement curve for a MFC with tempered steel shims, A325 bolts, one bolt at the weak end and two bolts at the strong end. The force displacement curve has two steps, and the first step and second step correspond to the force required to produce the sliding of the slotted plate (sliding strength) at the weak end and at the strong end, respectively. The stiffness for the first step is steep and it reduces slightly for the second step. The unloading stiffness is same as the initial stiffness. Figure 6 also shows that the sliding strength for the second step is twice the sliding strength for the first step. Thus, the ratio between the two sliding strengths, is the ratio between the number of bolts at the MFCs ends.

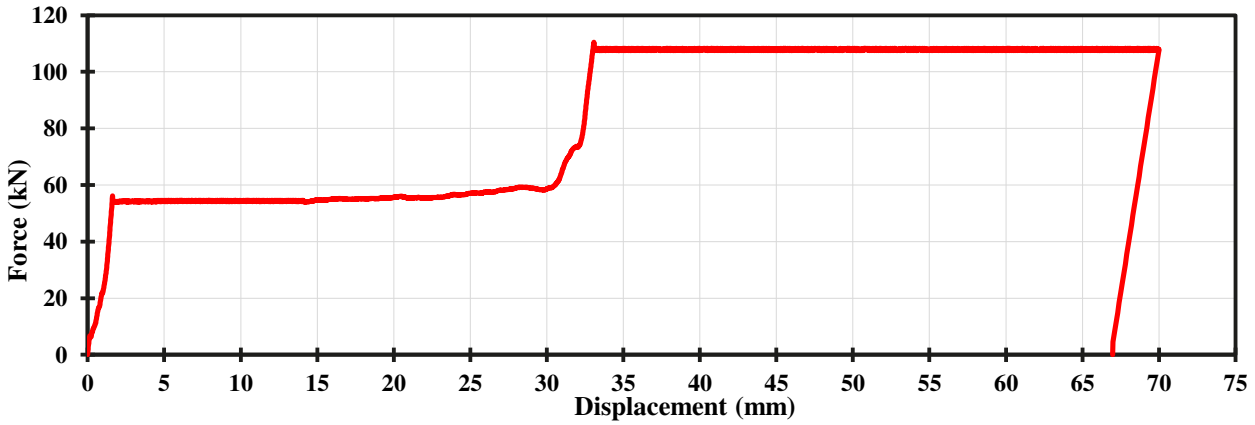

Figure 6: Monotonic tensile force – displacement curve for MFC with tempered steel shims, one A325 M16 bolt at the weak end and two A325 M16 bolts at the strong end

3.2 Sliding Mechanism

Figure 7 shows the sliding mechanism of a MFC with one bolt at the weak end and two bolts at the strong end. This sliding mechanism comprises 5 stages. In *Stage I*, the force increases stretching the MFC plates, but not producing any sliding on the MFC ends, as shown in Figure 7a. In *Stage II,* for a force equal to half of the MFC strength (P), the sliding of the slotted plate at the weak end is activated, and the force P remains constant while the slotted plate at the weak remains sliding, as shown in Figure 7b. In *Stage III,* the slotted plate at the weak end reaches the bolt shank and becomes on bearing on the bolt, thus the force increases above P, as shown in Figure 7b. In *Stage IV, for* a force equal to the full MFC strength ($2P$), the sliding of the slotted plate at the strong end is activated, and the force $2P$ remains constant while the slotted plate at the weak remains sliding, as shown in Figure 7c. In *Stage V*, the MFC is unloaded before the slotted plate at the strong end begins to bear on one of the bolts at the strong end.

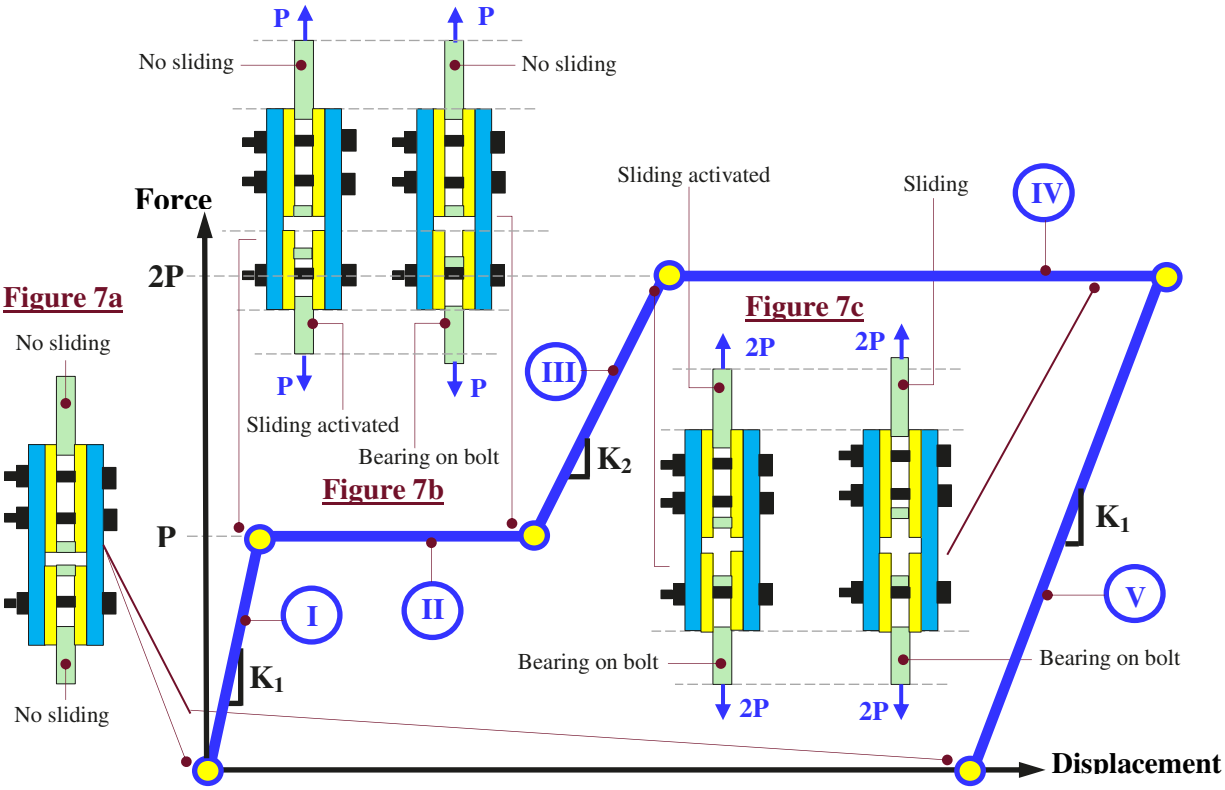

Figure 7: Sliding mechanism for MFCs (Internal view of slotted plates)

3.3 Material Friction Coefficient for A36 Steel – Tempered Steel Interfaces

Figure 8 shows the material friction coefficient μ obtained with Equation 1, and for a sliding plate of A36 steel and 5 tempered steel coupons. For each tempered steel coupon, two values of μ were obtained, thus a total of 10 values of μ were obtained for the same A36 steel sliding plate. Figure 8 shows μ for A36 steel – tempered steel interfaces varies in the range 0.21 – 0.40. The average value of μ for the 10 tests undertaken was 0.29.

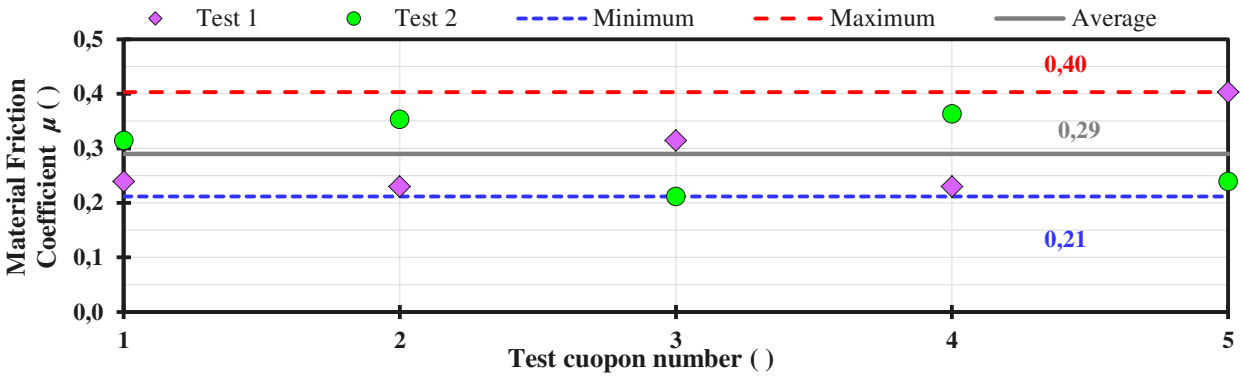

Figure 8: Material friction coefficient μ for A36 steel – tempered steel interfaces

4 PROPOSED FORCE - DISPLACEMENT MODEL

The proposed model for the monotonic tensile force - displacement curve of MFCs is defined in terms of the sliding force and the stiffness for the two steps of the curve, and it is based on experimental results. The sliding force, $F_{sliding}$, for the first and second loading steps can be calculated using the dry friction theory of Coulomb, and it can be expressed:

$$\boldsymbol{F_{sliding} = m \times n \times \mu \times F_{proof}} \tag{4}$$

Where, m is the number of bolts, n is the number of shear planes which is 2 in our case, μ is the material friction coefficient defined by Equation 1, and F_{proof} is the bolt proof load defined in Section 2.2.

The stiffness for the first loading step, K_1, can be calculated by coupling in series the axial stiffness of each slotted plate with the axial stiffness of the two fixed plates, and it can be expressed:

$$\boldsymbol{K_1 = \frac{1}{\frac{1}{k_{sw}} + \frac{1}{k_{ss}} + \frac{1}{k_f}}} \tag{6}$$

Where, k_{sw} is the axial stiffness of the slotted plate at the MFC weak end, k_{ss} is the axial stiffness of the slotted plate at the MFC strong end, and k_f is the axial stiffness of the two fixed plates. These axial stiffnesses are defined by Equation 2. In Equation 2, the plate length L for slotted plates corresponds to the distance from the unclamped end of the plate to the centroid of the MFC end (i.e., weak or strong). For the fixed plates, L corresponds to the distance between the centroid of the MFC ends.

The stiffness for the second loading step, K_2, can be calculated by coupling in series the stiffness for the first loading step K_1 with the bending stiffness of the bolt at the MFC weak end. The bending stiffness of the bolt at the MFC weak end is considered since the bolt shank is loaded by slotted plate after sliding half of the slot and bearing on the bolt as described in Sections 2.6 and 3.2. K_2 can be expressed:

$$\boldsymbol{K_2 = \frac{1}{\frac{1}{K_1} + \frac{1}{k_b}}} \tag{7}$$

Where, K_1 is the axial stiffness for the first loading step, and k_b is the bolt bending stiffness at the MFC weak end and defined in Section 2.6 by Equation 3. In Equation 6, the sliding of the slotted plate at weak end by half of the slot needs to be considered when assessing the axial stiffness of the slotted plate at the MFC weak

end $k_{sw.}$ It should be noted that the model above ignores the contribution of the shim shear stiffness, and the sliding of bolts across the bolt holes on the fixed plates.

5 EXPERIMENTAL DATA AND MODEL COMPARISON

Figure 9 shows a comparison between the experimental data and the proposed model for the monotonic tensile force - displacement curve of a MFC with tempered steel shims, A325 bolts, one bolt at the weak end and two bolts at the strong end. The experimental data corresponds to that presented in Figure 6, and the model was assessed with Equations 4 – 6 in Section 4. The sliding strengths for the first and second steps of the force – displacement curve model were calculated with Equation 4 and results are shown in Table 1. In Table 1, the value of μ corresponds to the average value reported in Section 3.3 for A36 steel – tempered steel interfaces, and the value of F_{proof} corresponds to that specified for A325 bolts by Research Council on Structural Connections 2000.

Table 1: Sliding strength for the first and second steps of the MFC force – displacement curve

		Number of bolts	Number of shear planes	Material friction coefficient	Bolt proof load	Sliding strength
		m	n	μ	F_{proof}	$F_{sliding}$
Force step	**Slotted plate sliding**	**#**	**#**	**----**	**kN**	**kN**
Fist	At weak end	1	2	0.29	85	49.3
Second	At strong end	2	2	0.29	85	98.6

The stiffnesses for the first and second steps of the force – displacement curve model, K_1 and K_2, were calculated with Equation 2, 3, 6 and 7, using an elastic modulus E=200kN/mm^2, and using the MFC dimensions shown in Figure 3b. Results from Equation 2, 3, 6 and 7 to get K_1 and K_2 are shown in Table2.

Table 2: Stiffness for the first and second steps of the MFC force – displacement curve

	Slotted plate - weak end			Slotted plate - strong end			Fixed plates			Bolt at weak end			
	Area	Length	Axial stiffness	Area	Length	Axial stiffness	* Area	Length	Axial* stiffness	Area	Length	Bending stiffness	MFC stiffness
Force step	A mm^2	L mm	k_{sw} kN/mm	A mm^2	L mm	k_{ss} kN/mm	A mm^2	L mm	k_f kN/mm	A mm^2	L mm	k_b kN/mm	K_i kN/mm
First	1120	190	1178.9	1120	250	896.0	2240	270	1659.3	201	58	------	389.6
Second	1120	225	995.6	1120	250	896.0	2240	270	1659.3	201	58	158.3	110.6

*Calculated for 2 fixed plates

Figure 9 shows a satisfactory agreement between the experimental data and the model. The sliding strengths predicted with the model vary between 83% - 90% of the experimental values. The predicted stiffness for the first loading step K_1 follows the initial trend of the experimental data, but as the displacements increase, the proposed model is stiffer than the experimental data. The predicted stiffness for the second loading step K_2 follows the final trend of the experimental data, but at the beginning of the second step, the proposed model is stiffer than the experimental data. These results indicate the model reasonably predicts the sliding strengths, and the stiffness model needs to be refined aiming to get a good agreement with the experimental data.

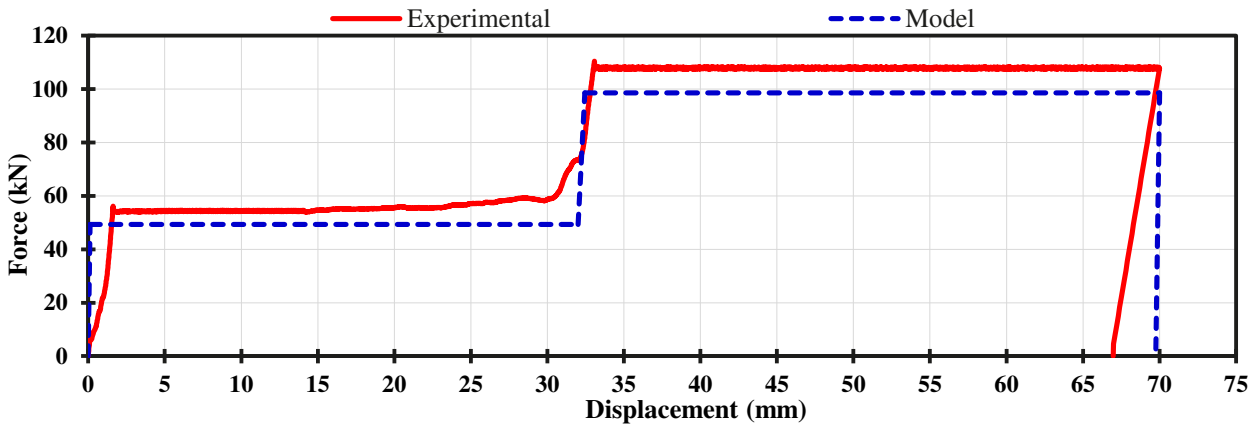

Figure 9: Experimental and model comparison for the monotonic tensile force-displacement curve for MFC with tempered steel shims, one A325 M16 bolt at the weak end and two A325 M16 bolts at the strong end

6 CONCLUSIONS

This paper describes the monotonic force – displacement curve for multistage friction connections, and proposes a simple model for predicting this curve. It was shown that:

i. MFCs can be used to dissipate seismic energy in beam to column joints or braces. MFCs comprise two co-linear symmetric friction connections, one assembled with less bolts than the other.

ii. The monotonic tensile force-displacement curve of MFCs has two steps representing the sliding of the slotted plates at the MFC ends. The ratio of the sliding strength for these steps is the ratio between the number of bolts at the MFCs ends. The stiffness for the first step is steep, and it reduces for the second step.

iii. The MFC sliding mechanism initially involves sliding the slotted plate at the weak end. The strength at this end increases when the bolt bears on the slotted plate. This causes further sliding to occur in the slotted plate at the strong end at a higher force

iv. The friction coefficient at the A36 steel – tempered steel shim interfaces under gravity loads varied between 0.21 and 0.40. In design, for these materials an average friction coefficient of 0.29 can be used.

v. A simple model to predict the sliding strengths and the stiffnesses of the MFCs tensile monotonic force - displacement curve was proposed. The model considers the Coulomb dry friction theory, the axial stiffness of the MFC plates, and the bending stiffness of the bolt at the MFC weak end. A satisfactory agreement between experimental data and the model was found.

7 REFERENCES

Chanchí Golondrino, J. C., MacRae, G. A., Chase, J. G., Rodgers, G. W., Clifton, G. C. 2020. Seismic Behaviour of Symmetric Friction Connections for Steel Buildings, *Engineering Structures,* Vol 224, DOI: https://doi.org/10.1016/j.engstruct.2020.111200

Chanchí Golondrino, J. C., Moreno Castañeda, B., Restrepo Botero, M. 2022. Site Surface Conditions Effects on the Static Friction Coefficient for Metallic Materials, *Journal of Construction Engineering*. Submitted and under review.

FitzGerald, T. F., Anagnos, T., Goodson, M., Zsutty, T. 1989. Slotted Bolted Connections in Seismic Design for Concentrically Braced Connections, *Earthquake Spectra*, 5 (2): 383-391, DOI: https://doi.org/10.1193/1.1585528

Grigorian, C.E. & Popov, E.P. 1994. Energy Dissipation with Slotted Bolted Connections, *Report UCB/EERC-94/02, Engineering Research Center College of Engineering.* University of California: Berkeley - USA.

MacRae, G. A. 1994. P-Δ Effects on Single-Degree-of-Freedom Structures in Earthquakes, *Earthquake Spectra,* Vol 10(3): 539-568, DOI: *https://doi.org/10.1193/1.1585788*

MacRae, G. A. 2021. Multistage Friction Connections – Idea Proposal, *Hera Innovation in Metals*.

Tremblay, R. 1993. Seismic Behaviour and Design of Friction Concentrically Braced Frames for Steel Buildings, *Unpublished PhD Thesis, Department of Civil and Environmental Engineering.* University of British Columbia: Vancouver, DOI: *https://dx.doi.org/10.14288/1.0050464.*

Xie, R., Chanchí Golondrino, J. C., MacRae, G. A., Clifton, G. C. 2018. Braced Frame Symmetrical and Asymmetrical Friction Connection Performance, *Key Engineering Materials*, Vol 763: 216-22*3, doi: https://doi.org/10.4028/www.scientific.net/KEM.763.216*.

Popov, V. L. (2) 2017. *Contact Mechanics and Friction, Physical Principles and Applications*. Springer: Berlin – Germany.

Research Council on Structural Connections. 2000. Specification for Structural Joints Using ASTM A325 or A490 Bolts, *RCSC Committee 15 – Specifications and approved by the Research Council on Structural Connections.*